Analysis and Optimization of a New Differentially-Driven Cable Parallel Robot

Hamed Khakpour
Mechanical Engineering Department
Ecole Polytechnique of Montreal
Montreal, QC, CANADA, H3T 1J4
Email: hamed.khakpour@polymtl.ca

Lionel Birglen
Mechanical Engineering Department
Ecole Polytechnique of Montreal
Montreal, QC, CANADA, H3T 1J4
Email: lionel.birglen@polymtl.ca

Souheil-Antoine Tahan
Mechanical Engineering Department
Ecole de technologie superieure
Montreal, QC, CANADA, H3C 1K3
Email: antoine.tahan@etsmtl.ca

In this paper, a new 3-DOF differentially-actuated cable parallel robot is proposed. This mechanism has a hybrid architecture and is driven by a prismatic actuator and three cable differentials. Through this design, the idea of using differentials in the structure of a spatial cable robot is investigated and their differences with architectures using individually-actuated cables are specified. Considering their particular properties, the kinematic analysis of the robot and the relationship between the actuation forces and the external wrench are presented. Then, two indices are defined to evaluate the wrench closure and wrench feasible workspaces of the robot. Using these indices, the robot is subsequently optimized. Finally, the performance of the optimized differentially-driven robot is compared with fully-actuated mechanisms. The results show that through a proper design methodology, the robot can have a larger workspace and better performance using differentials than the fully-driven cable robots using the same number of actuators.

Keywords: *cable robot, differential mechanism, kinematic analysis, workspace, optimization.*

1 Introduction

Due to the higher dexterity, larger payload and greater precision of parallel robots over common serial architectures, an abundant range of literature can be found dedicated to this class of robotic manipulators and many industrial applications are now common. These mechanisms are mainly categorized as either cable-driven or linkage-driven parallel robots [1]. Cable-driven manipulators are a particular class of parallel mechanisms where the moving platform (MP) is connected to the base platform (BP) through a set of cables [2].

Compared to linkage-driven designs, cable robots are usually less expensive, simpler, lighter, have low friction/inertia, and larger workspace [3–8]. Because of these properties, they can be used in areas where a dexterous machine with a very large reachable workspace is demanded [9]. Several cable robots are now commercialized and used in many fields (e.g., the ultrahigh speed robot Falcon [10], Skycam [11], NIST Robocrane [12], and Cablecam [13]). On the other hand, they suffer from the unilateral and limited force in the cables, are prone to vibrations, and the possibility of interferences among cables. These issues can weaken their capability to be used in some applications [4, 5, 9].

Since cables are flexible, they can only sustain tension but not compression [9]. Thus, n-DOF cable-driven robots should have at least n+1 cables to fully constrain and manipulate the MP [3, 10, 14]. It should be noted that, using more cables, one can expect better performance and larger workspace for these mechanisms as reported in the literature [7, 9]. The unilateral nature of cables also leads to some major differences between the criteria considered in the analysis of cable-driven and linkage-driven robots. One of them is the method of calculation of their workspaces [1, 5, 7, 9].

Previously, different properties of cable-driven mechanisms such as wrench closure and wrench feasible workspaces (WCW & WFW), arrangement and interference of cables were at the center of attention of many research initiatives. For instance, Pusey et al. [1] presented an incompletely restrained 6-6 cable-suspended robot and considered the global dexterity as an index (GDI) to optimize its workspace. Later, Fattah and

Agrawal [9] proposed a similar analysis for the optimal design of a cable-suspended planar robot, in which the GDI and the area of the workspace were used as indices to optimize the number of cables, size and geometry of the MP. Shiang et al. [15] analyzed the kinematic properties of a 3-DOF cable-suspended crane. In this study, the flexibility of cables was considered to obtain the equations of motion. Gouttefarde and Gosselin [8] developed an algorithm to find the wrench-closure and reachable workspaces of a planar cable robot. For this, several theorems were presented to define the WCW of this type of robot.

Also, Bouchard and Gosselin [2] introduced a geometrical approach to investigate the wrench-feasible (WF) property of cable robots with two to six DOFs. Mao and Agrawal [16] designed and manufactured a new 5-DOF cable-driven rehabilitation mechanism with adjustable cable connection points which has a light and compact structure. The workspace of this device was improved by optimizing the locations of the attachment points of all cables.

With all these robots, an actuation redundancy is necessary which significantly increases the cost and makes it harder to control the robots. In general, since the performances of these mechanisms are improved by employing more cables, these drawbacks become a painful burden. To overcome this issue, in this paper, a new 3-DOF cable-driven mechanism is proposed in which the MP is manipulated by three differentials instead of a set of independently actuated cables. The idea of using cable differentials in the structure of a planar cable robot was presented and investigated by the authors in [17]. In this paper, their impact on the performance of a spatial architecture is analyzed. The differentials considered in this paper are composed of two cables simultaneously driven by a single actuator through a differential mechanism. As described in [17] for planar cases, this technique can be generalized by using diverse numbers of cables with different arrangements while few actuators are considered. Through the comparison of this differentially-driven mechanism with fully actuated solutions the authors reveal that by using differentials in the structure of this robot, its performances are improved.

2 A New Differentially-driven Cable Robot

Differentials are widely used in many mechanical devices to resolve an actuation source into two outputs or combine two inputs into a single output. By definition, they have two degrees of freedom [18, 19]. Thus, to produce more outputs, they have to be connected together for instance in serial or parallel patterns [19]. Commonly used examples of these mechanisms are bevel gear differentials, planetary gear differential, seesaw mechanisms, and tendon-pulley arrangements [20].

To illustrate the difference between differentially actuated cables and independently driven ones, two planar

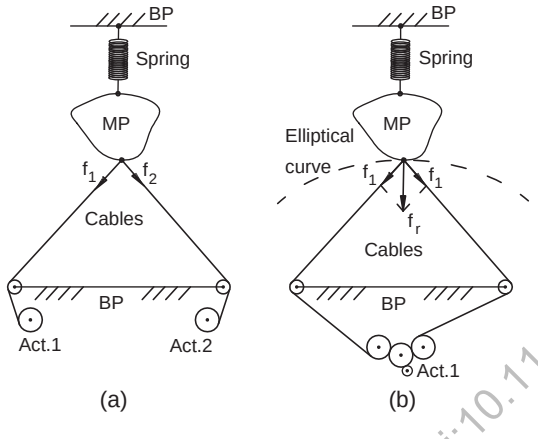

Fig. 1. Planar cable mechanisms actuated by (a) two independent cables; (b) two cables driven by a differential

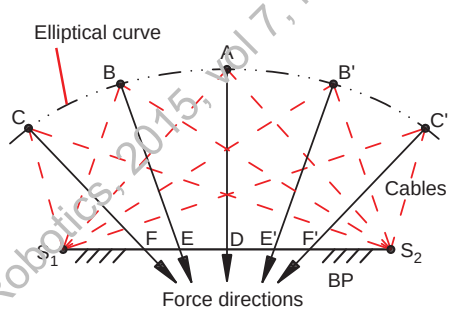

Fig. 2. Direction of resultant force of the two cables of a differential when its actuator is locked

cable mechanisms shown in Fig. 1 can be compared. In Fig. 1 (a), a pair of cables connecting the MP to the BP are controlled by two distinct actuators (the spring is only used to maintain the tension force in the cables). In this example, the cables and spring constrain the position of the MP. On the other hand, the cables of the differential system depicted in Fig. 1 (b) have dependent forces (with ideally equal magnitude). Thus, their resultant force lies on a particular line (ideally again, on the bisector of the two cables) and they can constrain the MP only in one direction. Consequently, the MP can move on a direction normal to this force. Therefore, if the actuator is locked, the attachment point of the cables on the MP will define an elliptical curve.

This property can be beneficial because, as illustrated in Fig. 2, the direction of the resultant force is always normal to the curve of an imaginary ellipse. When the attachments point of the cables on the MP lies on point A (equidistant of points S_1 and S_2), the direction of this force passes though the midpoint of line S_1S_2. Then, this system acts as a single cable connected at points A and D. On the other hand, if this attachment point moves away from point A (e.g., towards points B or C), the bisector of the two cables crosses the line S_1S_2 at points different than the midpoint D (e.g., points E

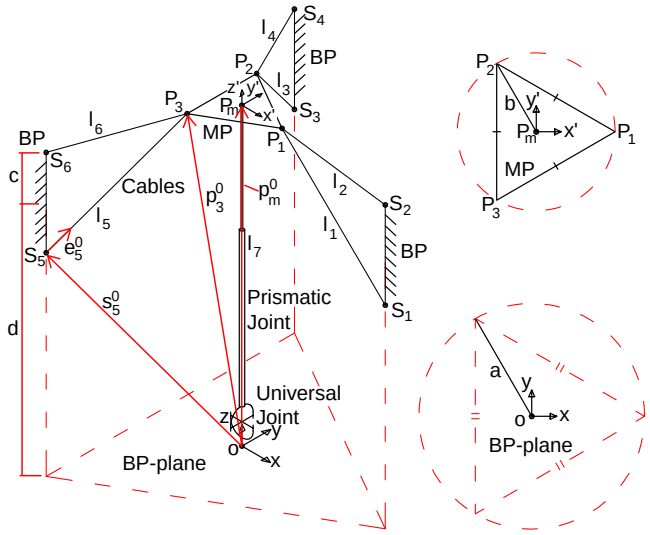

Fig. 3. Schematic of the proposed 3-DOF differential cable-driven robot

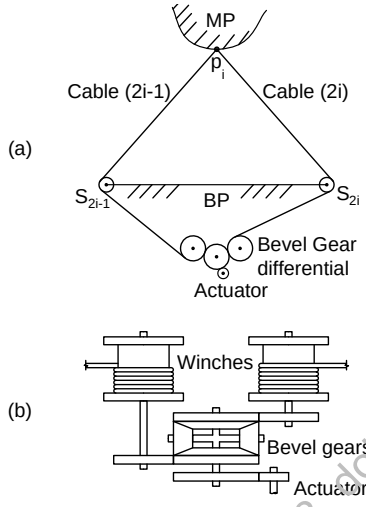

Fig. 4. Schematic of: (a) a differentially actuated cable system; (b) a typical bevel gear actuated differential

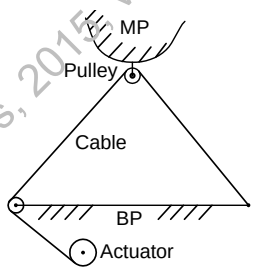

Fig. 5. Typical differential made of a cable and pulley system

or F). This gives a unique property to differentials when they are used in the structure of a cable driven robot, namely to have variable virtual attachment points on the BP.

The objective in designing a differentially-driven cable robot is to use differentially-driven cables in its architecture to fully constrain its MP while the number of the actuators is kept at minimum and more cables are used. In the presented mechanism, an actuated prismatic joint similar to the one presented in [21] is used to increase the stiffness of the robot and maintain the cable tensions. As illustrated in Fig. 3, this robot is cylindrically symmetric and the prismatic joint is connected to the BP through a passive universal joint. It is then rigidly connected to the MP in order for this robot to have 3-DOF. The cables of the three differentials are connecting the three vertices of the triangular MP to the virtual cylindrical surface on the BP along three lines parallel to the axis of this cylinder. Consequently, the robot has four actuators (three in the differentials and one in the prismatic joint) and is overconstrained.

In this robot, there are seven connections between the MP and the BP, namely a prismatic joint and six cables. These cables are driven by three differentials embedded in the BP at points $S_1 - S_2$, $S_3 - S_4$, and $S_5 - S_6$, so that point P_i is connected to points S_{2i-1} and S_{2i} via the cables $2i-1$ and $2i$. Note that the reason to select these pairs of cables to be differentially driven is to maximize certain characteristics (which will be specified later) related to the performance of this robot. Nevertheless, other pair of cables can also be chosen but the resulting performance would be actually weakened. The schematics of one of these three identical single differentials and its bevel gear mechanism are illustrated in Fig. 4. As can be seen in this figure, each differential has a single actuator installed in the BP and drives the two cables through a bevel gear differential mechanism while the other sides of the cables are attached to the MP. These three mechanisms are here referred to as $S_1 - P_1 - S_2$, $S_3 - P_2 - S_4$, and $S_5 - P_3 - S_6$.

It should be noted that, the introduced differential can also be replaced by other types of differentials. For example, a cable and pulley system can be used instead of the bevel gear differential in order for the cable to be attached to the BP at one end, passed through a pulley (which is attached to the MP), and then, connected to an actuator in the BP at its other end as illustrated in Fig. 5. In this case, the actuator just produces the tension of one side of the cable. But, due to the friction in the pulley, the tension of the cable is not equal in its two branches and therefore, the resultant force may not lay on the bisector of the two cables. Thus, from a kinematic point of view, this design yields uncertain practical performances and consequently, is not considered in this paper.

3 Kinematic Analysis of the robot

3.1 Direct and inverse kinematic problems

The first step in the analysis of the robot is to solve its direct and inverse kinematic problems (DKP & IKP).

For this, the position vectors of the attachment points of the cables on the BP with respect to the inertial frame (centered in O, cf. Fig. 3), $\mathbf{s}_j^0$ for $j=1,\cdots,6$, and on the MP with respect to the local frame (centered in P_m, cf. Fig. 3), $\mathbf{p}_i^m$ for $i=1,\ 2,\ 3$, are considered.

Then, the positions of points P_i^0 with respect to the inertial frame are found as:

$$\mathbf{p}_i^0 = \mathbf{R}_m^0 \mathbf{p}_i^m + \mathbf{p}_m^0 \quad \text{for } i=1,\ 2,\ 3, \tag{1}$$

where $\mathbf{p}_m^0 = [x,y,z]$ is the position vector of the center of the MP and $\mathbf{R}_m^0$ is the rotation matrix of the later expressed as $\mathbf{R}_m^0 = \mathbf{R}_x(\theta_1)\mathbf{R}_y(\theta_2)$, where $\mathbf{R}_x(\theta_1)$ and $\mathbf{R}_y(\theta_2)$ are respectively the rotation matrix around the x-axis of the inertial frame with an angle θ_1, and then, around the y-axis, with an angle θ_2, of the resulting frame attached to the universal joint.

By considering $\mathbf{e}_j$ for $j=1,\cdots,6$ as unit vectors along the cables from S_j to P_i defined in the inertial frame, and also knowing the position vector $\mathbf{p}_m^0$, the IKP is solved as:

$$\theta_1 = -atan2(z,y) \quad \text{where} \quad \theta_1 \in [-\pi,\pi], \tag{2a}$$

$$\theta_2 = \arcsin(\frac{x}{l_7}) \quad \text{where} \quad \theta_2 \in [-\frac{\pi}{2},\frac{\pi}{2}], \tag{2b}$$

$$l_j = \left\|\mathbf{s}_j^0 - \mathbf{p}_i^0\right\| \text{ for } \begin{cases} j=1,\ 2 \text{ if } i=1 \\ j=3,\ 4 \text{ if } i=2 \\ j=5,\ 6 \text{ if } i=3 \end{cases} \text{ and } l_7 = \left\|\mathbf{p}_m^0\right\|, \tag{2c}$$

$$l_{a1} = l_1 + l_2, \quad l_{a2} = l_3 + l_4, \quad l_{a3} = l_5 + l_6, \tag{2d}$$

where l_7 is the length of the prismatic joint, l_j for $j=1,\cdots,6$ is the length of the jth cable and l_{ai} for $i=1,\ 2,\ 3$ is the total length of the cables driven by the ith differential.

In the DKP, the total length of the cables of the differentials, l_{ai}, and the prismatic joint, l_7 are known and the position and orientation of the MP should be found. Since the robot is overconstrained, the DKP is defined by an over-determined system of equations. To solve this problem a numerical method such as a gradient descend method can be used.

3.2 Direct and inverse velocity problems

To obtain the relationships between the twist of the MP and the actuated joint rates, the Jacobian matrix of the robot must be defined. This matrix can be readily obtained by taking the derivatives of the position vectors $\mathbf{p}_i^0$. Knowing the twist of the MP at the point P_m, the inverse velocity problem (IVP) of this mechanism is solved as:

$$\begin{bmatrix} \dot{l}_1 \\ \dot{l}_2 \\ \dot{l}_3 \\ \dot{l}_4 \\ \dot{l}_5 \\ \dot{l}_6 \\ \dot{l}_7 \end{bmatrix} = \begin{bmatrix} \mathbf{e}_1^T & (\mathbf{p}_1^0 \times \mathbf{e}_1)^T \\ \mathbf{e}_2^T & (\mathbf{p}_1^0 \times \mathbf{e}_2)^T \\ \mathbf{e}_3^T & (\mathbf{p}_2^0 \times \mathbf{e}_3)^T \\ \mathbf{e}_4^T & (\mathbf{p}_2^0 \times \mathbf{e}_4)^T \\ \mathbf{e}_5^T & (\mathbf{p}_3^0 \times \mathbf{e}_5)^T \\ \mathbf{e}_6^T & (\mathbf{p}_3^0 \times \mathbf{e}_6)^T \\ \mathbf{e}_7^T & \mathbf{0}_{1\times 3} \end{bmatrix} \begin{bmatrix} \mathbf{v}^{\parallel} \\ \boldsymbol{\omega} \end{bmatrix} \leftrightarrow \dot{\mathbf{l}} = \mathbf{J}\mathbf{t}, \tag{3}$$

where $\dot{l}_j$ for $j=1,\cdots,7$ are the length change rates of the six cables and the prismatic joint; $\dot{\mathbf{l}}$ and $\mathbf{t}$ are respectively the vectors of the joint rates and the twist; $\mathbf{v}$ and $\boldsymbol{\omega}$ are respectively the linear and angular velocity vectors of the MP at the point P_m and $\mathbf{v}^{\parallel} = \mathbf{e}_7\mathbf{e}_7^T\mathbf{v}$. Since the robot only has 3 DOF, the vectors $\mathbf{v}$ and $\boldsymbol{\omega}$ are related. To find this, by projecting the vector $\mathbf{v}$ onto a plane with normal of $\mathbf{e}_7$ and calculating the derivative of position vector $\mathbf{p}_m = l_7\mathbf{e}_7$, the passive joint rates (in the universal joint) are obtained as:

$$\dot{\theta}_1 = \frac{\frac{-v_y^{\perp}}{l_7} + \dot{\theta}_2 s_{\theta_1} s_{\theta_2}}{c_{\theta_1} c_{\theta_2}} \quad \text{and} \quad \dot{\theta}_2 = \frac{v_x^{\perp}}{l_7 c_{\theta_2}}, \tag{4}$$

where $v_x^{\perp}$ and $v_y^{\perp}$ respectively denote x and y components of the vector $\mathbf{v}^{\perp} = (\mathbf{I}_{3\times 3} - \mathbf{e}_7\mathbf{e}_7^T)\mathbf{v}$. Next,the angular velocity is found as:

$$\boldsymbol{\omega} = \begin{bmatrix} \dot{\theta}_1 \\ \dot{\theta}_2 c_{\theta_1} \\ \dot{\theta}_2 s_{\theta_1} \end{bmatrix}. \tag{5}$$

The linear velocities of the actuators of the differentials (i.e., the displacement rates of the two cables of each differential) are then found as $\dot{\mathbf{l}}_a = \mathbf{T}\dot{\mathbf{l}}$ where $\dot{\mathbf{l}}_a = [\dot{l}_{a1}\ \dot{l}_{a2}\ \dot{l}_{a3}\ \dot{l}_7]^T$ is the vector of actuation rates and matrix $\mathbf{T}$ is found from Eq. (2d) as:

$$\mathbf{T} = \begin{bmatrix} 1 & 1 & 0 & 0 & 0 & 0 & 0 \\ 0 & 0 & 1 & 1 & 0 & 0 & 0 \\ 0 & 0 & 0 & 0 & 1 & 1 & 0 \\ 0 & 0 & 0 & 0 & 0 & 0 & 1 \end{bmatrix}. \tag{6}$$

Finally, the IVP can be solved as:

$$\begin{bmatrix} \dot{l}_{a1} \\ \dot{l}_{a2} \\ \dot{l}_{a3} \\ \dot{l}_7 \end{bmatrix} = \begin{bmatrix} \mathbf{e}_1^T + \mathbf{e}_2^T & (\mathbf{p}_1^0 \times (\mathbf{e}_1 + \mathbf{e}_2))^T \\ \mathbf{e}_3^T + \mathbf{e}_4^T & (\mathbf{p}_2^0 \times (\mathbf{e}_3 + \mathbf{e}_4))^T \\ \mathbf{e}_5^T + \mathbf{e}_6^T & (\mathbf{p}_3^0 \times (\mathbf{e}_5 + \mathbf{e}_6))^T \\ \mathbf{e}_7^T & \mathbf{0}_{1\times 3} \end{bmatrix} \begin{bmatrix} \mathbf{v}^{\parallel} \\ \boldsymbol{\omega} \end{bmatrix}. \tag{7}$$

The first matrix in the right hand side of Eq. (7) is referred to as a modified Jacobian, $\mathbf{J}_m$, particular to the proposed differential cable-driven robot.

The direct velocity problem (DVP) aims at finding the twist of the MP when the joint rates are known. Considering Eqs. (4), (5) and (7) and knowing the configuration of the robot, there are four equations and three unknowns (i.e., the components of $\mathbf{v}$). Therefore, if one of these equations is dependent to the others then there is a solution, otherwise, that vector of joint rates $\dot{\mathbf{l}}$ is deemed not feasible.

3.3 Actuation forces and output wrench relationships

The tension matrix of a cable robot is defined as $\mathbf{A}=\mathbf{J}^T$ [9]. Using the principle of virtual work the relationship between the forces in the cables and the prismatic joint of the robot and the corresponding wrench at its MP is:

$$\mathbf{A}\mathbf{f}=\mathbf{w}, \tag{8}$$

where $\mathbf{f}$ and $\mathbf{w}$ are respectively the vectors describing the tension forces and the wrench. They are defined as:

$$\mathbf{f}=\begin{bmatrix}t_1 & t_2 & t_3 & t_4 & t_5 & t_6 & t_7\end{bmatrix}^T \quad \text{and} \quad \mathbf{w}=\begin{bmatrix}\mathbf{f}_w^T & \mathbf{n}_w^T\end{bmatrix}^T, \tag{9}$$

where t_j for $j=1,\cdots,6$ is the magnitude of the force in the j^{th} cable and t_7 is the magnitude of the force in the prismatic joint. Also, $\mathbf{f}_w$ and $\mathbf{n}_w$ are respectively the vectors of force and torque exerted to the MP at the point P_m. In a frictionless ideal case, the bevel gear system can produce equal tensions on both cables in each differential, i.e., $t_1=t_2$, $t_3=t_4$ and $t_5=t_6$. Consequently, vector $\mathbf{f}$ can be changed to $\mathbf{f}=\begin{bmatrix}t_1 & t_1 & t_3 & t_3 & t_5 & t_5 & t_7\end{bmatrix}^T$.

The total torque to be generated by the actuators of the differentials are $\tau_{a1}=2r_g t_1$, $\tau_{a2}=2r_g t_3$, and $\tau_{a3}=2r_g t_5$ where r_g is the gear ratio. Additionally, with this robot, the resultant force of the cables of each differential is considered to characterize its performance. Therefore, similar to the velocity problem and using the modified Jacobian, Eq. (8) is changed to:

$$\mathbf{A}_m\mathbf{f}_m=\mathbf{w}, \tag{10}$$

where $\mathbf{A}_m=\mathbf{J}_m^T$ and $\mathbf{f}_m=[t_1\ t_3\ t_5\ t_7]^T$. This robot is a 3-DOF mechanism (with two rotations and one translation) and works in a three dimensional space. On the other hand, an external wrench imposed to this robot as well as the resultant force and torque generated by the three differentials and the prismatic joint can have arbitrary directions. Indeed, considering the constraint exerted by the universal joint to the MP, the wrench that should be resisted by the actuators is limited to a force in the direction of $\mathbf{e}_7$ and a torque on a plane created by two cross axes of the universal joint with a normal defined as $\mathbf{e}_U=\begin{bmatrix}0 & -s\theta_1 & c\theta_1\end{bmatrix}^T$ [22]. Therefore, to eliminate the components of the force and torque vectors which are passively resisted by the universal joint not the actuators, they are projected to the relevant directions using the matrix $\mathbf{C}$ defined as:

$$\mathbf{C}=\begin{bmatrix}\mathbf{e}_7\mathbf{e}_7^T & \mathbf{0}_{3\times3}\\ \mathbf{0}_{3\times3} & \mathbf{I}_{3\times3}-\mathbf{e}_U\mathbf{e}_U^T\end{bmatrix}_{6\times6}. \tag{11}$$

Then, if the vector $\mathbf{f}_m$ is known, by using the matrix $\mathbf{C}$, the left hand side of Eq. (10) is projected onto the specific directions so that the vector $\mathbf{w}$ which is not compensated by the passive reaction of the universal joint is found as:

$$\mathbf{C}\mathbf{A}_m\mathbf{f}_m=\mathbf{w}. \tag{12}$$

On the other hand, if an arbitrary external wrench vector, $\mathbf{w}_a$, is exerted to the MP and the vector $\mathbf{f}_m$ is to be found, this wrench should be first mapped into the directions controlled by the actuators, namely:

$$\mathbf{A}_m\mathbf{f}_m=\mathbf{C}\mathbf{w}_a. \tag{13}$$

In Eqs. (12) and (13), the projection matrix $\mathbf{C}$ is used to take into account the components of the vectors of these equations in the actuated directions. Thus, one cannot compute any of these equations from the other. Any vector which has the same component in these directions would be a possible solution for these equations (either the generated wrench on the MP on the right hand side of Eq. (12) or the cable tensions in the left hand side of Eq. (13)). The other components of these vectors are resisted by the passive support of the robot.

Finding the resultant wrench using Eq. (12) is straightforward while in Eq. (13), there appears to be six equations and four variables. However, due to the constraints of the robot, there are only three independent equations. Therefore, this is an underdetermined system of equations. To solve this problem the WF condition is used. In this approach, it is assumed that one of the variables is known. Then, the three other variables are parametrically calculated. Next, the minimal and maximal allowed tensions in the cables are considered so that the minimum value is set for a cable which has the lowest tension while the tensions of the others should not exceed the maximum value. If such a force vector $\mathbf{f}_m$ is found, then, that wrench can be resisted by this robot.

The support of the robot (constituted by the universal joint) must be able to resist all the forces and torques applied by the actuators as well as an external wrench. To calculate this, it is assumed that an arbitrary wrench $\mathbf{w}_a$ is exerted to the MP and the actuation force vector $\mathbf{f}_m$ is found from Eq. (13). Then, the wrench imposed

to the support is found as:

$$\mathbf{w}_s = \mathbf{C}'(\mathbf{w}_a - \mathbf{A}_m \mathbf{f}_m) + \begin{bmatrix} t_7 \mathbf{e}_7 \\ \mathbf{0}_{3\times 1} \end{bmatrix}. \quad (14)$$

The support wrench vector $\mathbf{w}_s$ and the projection matrix $\mathbf{C}'$ are defined as:

$$\mathbf{w}_s = \begin{bmatrix} \mathbf{f}_s^T & \mathbf{n}_s^T \end{bmatrix}^T, \quad (15)$$

$$\mathbf{C}' = \begin{bmatrix} \mathbf{I}_{3\times 3} & \mathbf{0}_{3\times 3} \\ \mathbf{0}_{3\times 3} & \mathbf{e}_U \mathbf{e}_U^T \end{bmatrix}_{6\times 6}, \quad (16)$$

where $\mathbf{f}_s$ and $\mathbf{n}_s$ are respectively the vectors of resultant force and torque exerted to the support of the robot.

3.4 Workspace of the robot

Usually in the literature, two types of workspaces are defined for a cable-driven robot i.e., the WCW and WFW [5]. The WCW is a volume where the MP of the robot can be located and regardless of the exerted wrench, all its cables are in tension. The WFW is a subset of WCW where all cable tensions are within a specified range.

To find the WCW of the proposed robot, the distribution of the forces and torques produced by the actuators onto its MP must be investigated. These force/torque vectors should be able to span all directions in the considered n-D force/torque workspace to be able to produce any arbitrary wrench. To evaluate this for the forces, the unit vectors along the resultant force vector created by each differential at the MP and the prismatic joint (which can be either under compression or tension) are used to define a convex polyhedron. The starting points of these vectors are attached to the origin of the force workspace and their end points define the vertices of this polyhedron. Then, all these vertices are mapped onto a line which passes through the origin of this space and is parallel to $\mathbf{e}_7$ (i.e. $\Re^3 \to \Re^1$). If the origin is located between the two projected vertices most far apart, then, the robot can generate any arbitrary force along $\mathbf{e}_7$ in that specific configuration. The four unit vectors are:

$$\mathbf{u}_i = -\frac{\mathbf{e}_{2i-1}+\mathbf{e}_{2i}}{\|\mathbf{e}_{2i-1}+\mathbf{e}_{2i}\|} \text{ for } i=1,\,2,\,3 \text{ and } \mathbf{u}_4 = \beta \mathbf{e}_7, \quad (17)$$

where $\beta = -1$ or 1 depending on the direction of the force in the prismatic joint for each configuration of the robot. In the same way, by considering the unit vectors along the resultant torque vectors of the differentials (the prismatic joint cannot exert any torque on the MP) and projecting them onto a plane with normal $\mathbf{e}_U$, the wrench closure (WC) condition can be investigated for the torques. The unit vectors are defined by:

$$\mathbf{v}_i = \frac{\mathbf{p}_i^0 \times \mathbf{e}_{2i-1} + \mathbf{p}_i^0 \times \mathbf{e}_{2i}}{\left\|\mathbf{p}_i^0 \times \mathbf{e}_{2i-1} + \mathbf{p}_i^0 \times \mathbf{e}_{2i}\right\|} \quad \text{for} \quad i=1,\,2,\,3. \quad (18)$$

To check the WC condition for the forces in each pose of the robot, first the vectors $\mathbf{u}_i' = \mathbf{e}_7 \mathbf{e}_7^T \mathbf{u}_i$ for $i = 1, \cdots, 4$ are obtained. Then, the dot products $h_i = \mathbf{e}_7^T \mathbf{u}_i'$ for $i = 1, \cdots, 4$ are calculated. Next, if there is at least one change in the sign of h_i then, the force-closure condition is satisfied. For the torques, first, the mapped vectors $\mathbf{v}_i' = (\mathbf{I}_{3\times 3} - \mathbf{e}_U \mathbf{e}_U^T)\mathbf{v}_i$ are computed. Afterwards, a procedure similar to the one introduced in [5] is used. Namely, the cross product of the unit vectors $\mathbf{v}_i'$ are obtained as $\mathbf{m}_{ij} = \mathbf{v}_i' \times \mathbf{v}_j'$ for $i, j = 1,\,2,\,3$ and $i \neq j$. Then, $k_{ij} = \mathbf{e}_U^T \mathbf{m}_{ij}$ is calculated. Finally, if for each $\mathbf{m}_{ij}$ there is at least one change in the sign of k_{ij}, then, this condition is satisfied and if this happens simultaneously for both the force and torque vectors, that configuration belongs to the WCW of this robot.

To obtain the WFW, a geometrical method similar to the one proposed in [2] is used. This procedure is again implemented separately for the force and the torque vectors. For the force analysis, the tensions of all cables are desired to be between t_{min} and t_{max}. Then, vectors $\Delta \mathbf{t}_i = -(t_{max} - t_{min})(\mathbf{e}_{2i-1} + \mathbf{e}_{2i})$ for $i = 1,\,2,\,3$ and $\Delta \mathbf{t}_4 = \beta(t_{max}' - t_{min}')\mathbf{e}_7$ are considered respectively for the three differentials and the prismatic joint. Afterwards, similarly to the vectors $\mathbf{u}_i$, the vectors $\Delta \mathbf{t}_i$ are projected onto the direction of the vector $\mathbf{e}_7$ as $\Delta \mathbf{t}_i' = \mathbf{e}_7 \mathbf{e}_7^T \Delta \mathbf{t}_i$ for $i = 1, \cdots, 4$. Next, these vectors are used to generate a zonotope (a convex polytope with parallel edges [2]) which here is turned to a line segment and is used to calculate the WFW of the robot.

To produce this zone, first, the vectors $\Delta \mathbf{t}_i'$ for $i = 1, \cdots, 4$ are considered as a set of line segments. Next, their Minkowski sum [2] is calculated. Then, the vectors $\mathbf{t}_{i^{min}} = -t_{min}(\mathbf{e}_{2i-1} + \mathbf{e}_{2i})$ for $i = 1,\,2,\,3$ and $\mathbf{t}_{4^{min}} = \beta t_{min}' \mathbf{e}_7$ are used to modify the zonotope and obtain its final shape. The zone inside this polytope is found as [2]:

$$Z_f = \alpha_1 \Delta \mathbf{t}_1' \oplus \alpha_2 \Delta \mathbf{t}_2' \oplus \cdots \oplus \alpha_4 \Delta \mathbf{t}_4' + \sum_{i=1}^{4} \mathbf{e}_7 \mathbf{e}_7^T \mathbf{t}_{i^{min}}, \quad (19)$$

where $\alpha_i \in [0, 1]$ for $i = 1, \cdots, 4$, and the symbol $\oplus$ represents the Minkowski sum of line segments. Finally, the magnitude of the largest force vector that can be located in any direction inside this one-dimensional zone while its origin coincides with the origin of the zone, is the magnitude of the maximal allowable force.

A similar procedure is followed to obtain the maximal permissible torque. For this, vectors $\Delta \boldsymbol{\tau}_i = (t_{max} - t_{min})\mathbf{p}_i^0 \times (\mathbf{e}_{2i-1} + \mathbf{e}_{2i})$ for $i = 1,\,2,\,3$ are calculated and similar to the vectors $\mathbf{v}_i$, they are projected onto a plane with normal $\mathbf{e}_U$ as $\Delta \boldsymbol{\tau}_i' = (\mathbf{I}_{3\times 3} - \mathbf{e}_U \mathbf{e}_U^T)\Delta \boldsymbol{\tau}_i$ to create a two

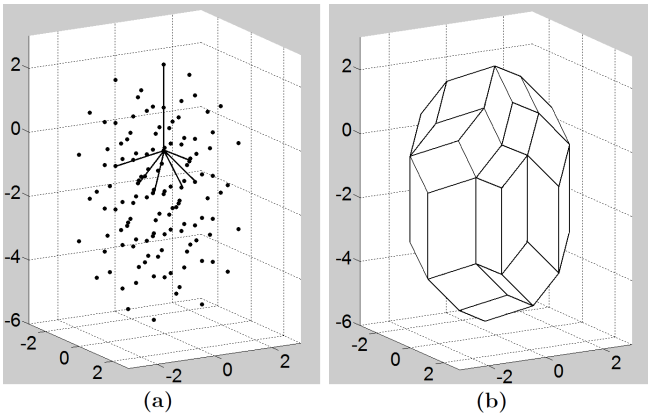

Fig. 6. (a) Seven line segments representing the base vectors of the zonotope and all nodes created by Minkowski sum of these lines; (b) Zonotope made of the nodes creating the boundary of the zone

dimensional zonotope. At the end, the final location of this geometry is obtained by using the vectors of minimal torques as $\tau_{i^{min}} = t_{min}\mathbf{p}_i^0 \times (\mathbf{e}_{2i-1} + \mathbf{e}_{2i})$ for $i = 1, 2, 3$. This two-dimensional zone is defined by:

$$Z_\tau = \gamma_1 \Delta\tau_1' \oplus \gamma_2 \Delta\tau_2' \oplus \gamma_3 \Delta\tau_3' + \sum_{i=1}^{3} (\mathbf{I}_{3\times 3} - \mathbf{e}_U \mathbf{e}_U^T)\tau_{i^{min}}, \quad (20)$$

where $\gamma_i \in [0,1]$ for $i = 1, 2, 3$. Finally, the radius of the largest circle which can be located inside the resultant two dimensional polytope with its center fixed to the origin of the geometry, is the magnitude of the maximum torque that can be resisted by the mechanism. If the maximum magnitude of both force and torque are larger than their specified minimally allowable values, then, that pose belongs to the WFW of the robot. In Fig. 6, an example of a three-dimensional zonotope created by seven vectors is presented.

4 Defining the characteristic indices

The proposed robot is assumed to work in a cylindrical workspace with a radius r_c and a height h_c. As shown in Fig. 7, the base of this cylinder is parallel to the BP plane and is located at a distance d_c from it. To optimize the performance of this robot, different aspects of its performance should be measured. In this paper, two measures are taken into account, namely, the size of the WCW and WFW. The investigation of these properties is performed via defining two dimensionless indices.

WCW: evaluated by an index I_{WCW}. This index is defined as the ratio between the volume of the conceptual cylinder and the sum of the volumes of this cylinder and the WCW of the robot, namely:

$$I_{WCW} = \frac{c}{c+q}, \quad (21)$$

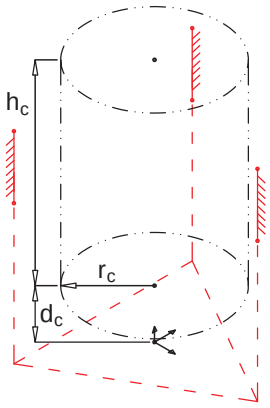

Fig. 7. Conceptual cylinder representing the volume in which the robot works

Table 1. Values of all parameters used in the optimization process

Parameters	Values	Parameters	Values
a	60 cm	t_{min}	10 N
d	90 cm	t_{max}	100 N
r_c	40 cm	t'_{min}	0 N
h_c	120 cm	t'_{max}	600 N
d_c	30 cm	f_{min}	400 N
		n_{min}	90 $N.m$
a_1	3	Range for b	[5,30] cm
a_2	1	Range for c	[0,60] cm

where c and q are the volume of respectively the cylinder and the WCW.

WFW: measured by the index I_{WFW} which is defined as:

$$I_{WFW} = \frac{c}{c+m}\left(\frac{f_{min}}{f_{min} + \frac{1}{m}\int_m f_i dv} + \frac{n_{min}}{n_{min} + \frac{1}{m}\int_m n_i dv}\right), \quad (22)$$

where m is the volume of the WFW; f_i and n_i are respectively the maximum feasible force and torque for each position of the MP in the WFW; also, f_{min} and n_{min} are respectively the specified minimal amount of force and torque the robot should be able to resist inside its WFW. The terms inside the parentheses in Eq. (22) show the normalized ratios between f_{min}/n_{min} and the average values of the maximum feasible force/torque inside the WFW. This index considers both the volume of the WFW and the magnitude of the maximal permissible force and torque for all points in this workspace.

5 Optimization and the results

The main objective in the optimization of the robot is to improve the performance of its three differentials to have a larger workspace. For this, the two indices

Table 2. Resultants of the optimization process

Variables	Values	Dimensions
c	16.51	cm
b	5.00	cm

and the conceptual cylinder are used to obtain the best set of design parameters. With this robot, the dimensions of the BP, i.e., a and d are assumed to be fixed while the dimension of the MP and the distance between two points of each differential (i.e. S_{2i-1} and S_{2i} for $i=1, 2, 3$), respectively b and c are to be found (c.f. Fig. 3). Considering the design limits of the robot, two boundaries are considered for these two goal parameters. In this process, the objective function to be minimized is defined as:

$$F_{GA} = a_1 I_{WCW} + a_2 I_{WFW} \ , \tag{23}$$

where a_1 and a_2 are weight coefficients. The input parameters of the optimization procedure re the dimensions of the conceptual cylinder and the BP, the boundaries of the cables tensions and the force in the prismatic joint, and finally the minimum amount of force and torque the robot should resist inside its WFW.

To optimize this robot, a genetic algorithm (GA) which is embedded in a commercial numerical software is used. The chosen values of all input parameters and the boundaries are presented in Table 1.

Since the WFW is a subset of the WCW and its volume depends on the minimum permissible force f_{min} and torque n_{min} (which are user defined parameters), with larger WCW the robot has the potential of having bigger WFW. Therefore, in this paper, a larger weight coefficient is considered for the WCW in the objective function.

Considering all these values, a GA with 120 individuals and 100 generations is run. The results of the optimization are presented in Table 2 and the schematic of the optimized robot in an arbitrary position inside its workspace is illustrated in Fig. 8.

As can be seen in Table 2, the GA found the best value for b exactly at the lower boundary. The same optimization with no boundary for b shows that this value is close to zero which is physically impractical. The reason for this is that in the areas of the cylinder close to each of the differentials, with smaller value of b, there is a smaller angle between the cables of that differential and so these cables can produce larger resultant force. Thus, the get rid of this problem a minimum boundary is considered.

Finally, this optimization reveals that the effects of using differential in a cable robot is a trade off between the expansion of the range of changes in the direction

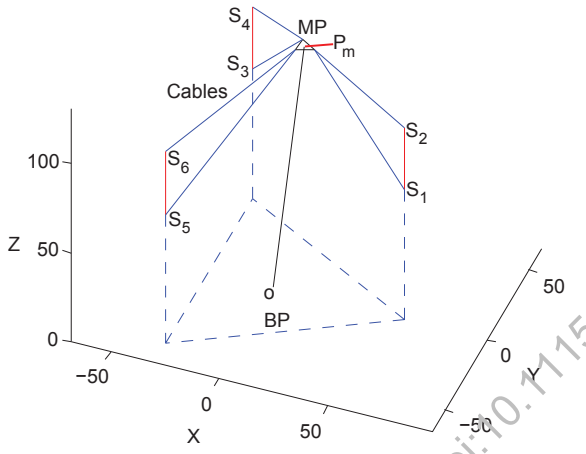

Fig. 8. Schematic of the optimized robot in an arbitrary location inside its workspace

of resultant force vector of each differential (which improves the both WCW and WFW) and the increase of the angle between their cables (which weakens the maximum value of the resultant force and so decreases the WFW).

6 Comparing the proposed differential cable robot with two fully actuated ones

In this section, to investigate the effect of using differentials in the structure of a cable robot, the optimized differentially actuated robot, referred to as 6-3-differential (with 6 cables and 3 actuators), is first compared with two fully actuated designs. The first mechanism has an architecture similar to the proposed robot but it is driven by three single cables instead of three differentials. The schematic of this robot which is here referred to as 3-3-full is illustrated in Fig. 9. The second fully actuated robot, called 6-6-full, has the same structure as the differential cable robot shown in Fig. 3, but all its cables are independently actuated.

This comparison is implemented for the two workspaces (WCW and WFW) of these robots. To do this, by taking the parameters of Tables 1 and 2 , the indices I_{WCW} and I_{WFW} as well as the ratios between the volumes of these workspaces (i.e. respectively v_{WCW} and v_{WFW}) and the volume of the cylinder v_c are measured and the results are presented in Table 3.

As can be seen in this table, with the same values for the design parameters, the two indices of the 6-3-differential cable robot are smaller (i.e. better) than the ones of the 3-3-full mechanism. This means that using differentials, while the number of actuators are kept at minimum (three in this case) one can expect a larger wrench closure and wrench feasible workspaces (which can also be seen as the ratios $\frac{v_{WCW}}{v_c}$ and $\frac{v_{WFW}}{v_c}$ in Table 3). This improvement is obtained as a result of two phenomena, i.e.:

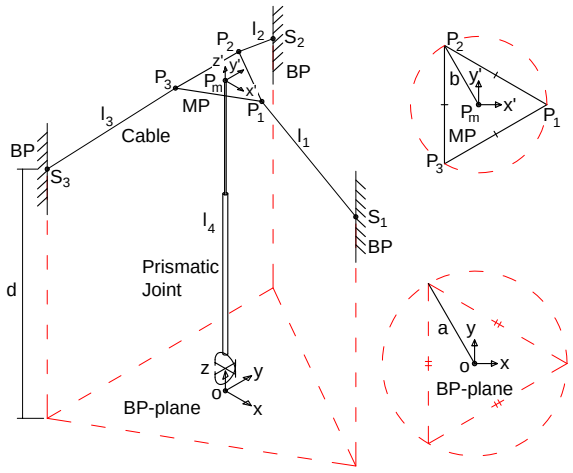

Fig. 9. Schematic of the 3-3-full cable robot with three independently actuated cables

Table 3. Comparing the performance of differential cable-driven robot with other mechanisms

Robot type	WCW		WFW	
	I_{WCW}	$\frac{v_{WCW}}{v_c}$	I_{WFW}	$\frac{v_{WFW}}{v_c}$
3-3-full cable robot	0.6194	0.6146	2	0
6-3-double cable robot	0.6194	0.6146	0.8473	0.0710
6-3-differential cable robot	0.6157	0.6241	0.8499	0.0705
6-6-full cable robot	0.5855	0.7081	0.8463	0.0731

1. The capability of using more cables with the same actuator via differentials;
2. The change in the direction of the resultant force of the cables of each differential (c.f. Fig. 2).

On the other hand, as one expected, these indices are even smaller with the 6-6-full robot than with the differentially actuated one. This shows that although the same number of cables is used in both architectures, due to the limits in the direction of the resultant force of the differentials, the 6-3-differential robot cannot have workspaces as large as the fully actuated one.

Next, a similar comparison is done between the optimized robot and another fully actuated mechanism which is here referred to as 6-3-double cable robot with the same architecture of 3-3-full but with two parallel cables attached to each other (to account for a thicker cable), i.e. $c = 0$. The results of this comparison are shown in Table 3. It seems that the optimized robot has a larger WCW but smaller WFW. Because in the 6-3-double mechanism, the angle between two cables is always zero and the magnitude of the resultant force is the scalar sum of the forces of the two cables. Nevertheless, as previously discussed, having greater WCW is more important than having larger WFW. Besides, the concept of using differential can also be valid for 3-3-double cable robot so that by using the cable and pulley differential presented in Fig. 5 one can increase the load capacity of the robot while the kinematic properties of the mechanism is the same as the 3-3-full manipulator.

7 Conclusions

This paper proposed a new 3-DOF cable parallel robot which is actuated by differentials instead of independent cables. This robot has a hybrid structure in which the MP is driven by four actuators, one is a prismatic joint and three others are connected to three differentials to drive six cables. For this, first the effects of using differentials on the forces exerted by the six cables on the MP were investigated. It was shown that, instead of the force and torque vectors produced by each single cable, the resultant force and torque vectors of the cables of each differential should be used. Next, the kinematic analysis of the robot was presented. Afterwards, to evaluate the two workspaces of the robot, the indices I_{WCW} and I_{WFW} were defined. By implementing the Genetic algorithm method and considering these indices, the performance of the robot was optimized. Then, the workspaces of the optimized differentially-driven robot were compared with the ones of fully actuated mechanisms. The results showed that through a proper design and using differentials, the robot can have larger WCW and WFW with respect to the mechanism with the same number of actuators driving independent cables.

References

[1] Pusey, J., Fattah, A., Agrawal, S., Messina, E., and Jacoff, A., 2003, "Design and Workspace Analysis of a 6-6 Cable-Suspended Parallel Robot", IEEE Int Conf Intell Rob Syst, Las Vegas, USA, Oct. 27-31, pp. 2090–2095.

[2] Bouchard, S., Gosselin, C.M., and Moore, B., 2010, "On the ability of a cable-driven robot to generate a prescribed set of wrenches", J. Mech. Rob., **2**(1), pp. 011010 (1-10).

[3] Perreault, S. and Gosselin, C.M., 2008, "Cable-driven parallel mechanisms-application to a locomotion interface", J Mech Des, Trans ASME, **130**(10), pp. 1023011–1023018.

[4] Tadokoro, S., Murao, Y., Hiller, M., Murata, R., Kohkawa, H., and Matsushima, T., 2002, "A motion base with 6-DOF by parallel cable drive architecture", IEEE ASME Trans Mechatron, **7**(2), pp. 115–123.

[5] Yang, G., Pham, C.B., and Yeo, S.H., 2006, "Workspace performance optimization of fully restrained cable-driven parallel manipulators", IEEE Int Conf Intell Rob Syst, Beijing, China, Oct. 9-15, pp. 85–90, .

[6] Ferlay, F. and Gosselin, F., 2008, "A new cable-actuated Haptic interface design", Devices and Scenarios - 6th International Conference EuroHaptics, Madrid, Spain, Jun. 10-13, pp. 474–483.

[7] Yang, G., Lin, W., Kurbanhusen, M.S., Pham, C.B.,

and Yeo, S.H., 2005, "Kinematic Design of a 7-DOF Cable-Driven Humanoid Arm: A Solution-in-nature Approach", IEEE ASME Int Conf Adv Intellig Mechatron AIM, California, USA, Jul. 24-28, pp. 444–449.

[8] Gouttefarde, M. and Gosselin, C.M., 2006, "Analysis of the wrench-closure workspace of planar parallel cable-driven mechanisms", IEEE Trans. Robot., **22**(3), pp. 434–445.

[9] Fattah, A. and Agrawal, S.K., 2005, "On the design of cable-suspended planar parallel robots", J Mech Des, Trans ASME, **127**(5), pp. 1021–1028.

[10] Kawamura, S., Choe, W., Tanaka, S., and Pandian, S.R., 1995, "Development of an ultrahigh speed robot FALCON using wire drive system", Proc IEEE Int Conf Rob Autom, Nagoya, Japan, May 21-27, pp. 215–220.

[11] Brown, G.W., 1984, "Improved suspension system for supporting and conveying equipment, such as a camera", US Patent No. 4 710 819.

[12] Albus, J., Bostelman, R., and Dagalakis, N., 1993, "The NIST ROBOCRANE", J. Robot. Syst., **10**(5), pp. 709–724.

[13] Rodnunsky, J., 2006, "Cabling system and method for facilitating fluid three-dimensional movement of a suspended camera", US Patent No. 7 088 071.

[14] Carricato, M. and Merlet, J.P., 2013, "Stability analysis of underconstrained cable-driven parallel robots", IEEE Trans. Robot., **29**(1), pp. 288–296.

[15] Shiang, W.J., Cannon, D., and Gorman, J., 2000, "Optimal force distribution applied to a robotic crane with flexible cables", Proc IEEE Int Conf Rob Autom, San Francisco, USA, Apr. 24-28, pp. 1948–1954.

[16] Mao, Y. and Agrawal, S.K., 2011, "A cable driven upper arm exoskeleton for upper extremity rehabilitation", Proc IEEE Int Conf Rob Autom, Shanghai, China, May 9-13, pp. 4163–4168.

[17] Khakpour, H., Birglen, L., and Tahan, S. A., 2014, "Synthesis of differentially driven planar cable parallel manipulators", IEEE Trans. Robot. [article in press]

[18] IFToMM Commission A, 1991, "Terminology for the Theory of Machines and Mechanisms", Mech. Mach. Theory, **26**(5), pp. 435–539, .

[19] Hirose, S., 1985, "Connected differential mechanism and its applications: robotic manipulator", Proceedings of International Conference on Advanced Robotics, Tokyo, Japan, Sep. 9-10, pp. 319–326.

[20] Birglen, L., Laliberte, T., and Gosselin, C., 2008, *Underactuated Robotic Hands*, Springer-Verlag, New York, vol. 40.

[21] Landsberger, S. and Sheridan, T. 1987, "Parallel link manipulators", US Patent No. 4 666 362

[22] Carricato, M and Gosselin, C., 2009, "On the Modeling of Leg Constraints in the Dynamic Analysis of Gough/Stewart-Type Platforms", J. Comput. Nonlinear Dyn., **4**(1), pp. 1–8.